Characterization of a diagnostic Fab fragment binding trimeric Lewis X

Geus, D.C. de; Thomassen, E.A.J.; Hokke, C.H.; Deelder, A.M.; Abrahams, J.P.; Roon, A.M. van

PROTEINS
STRUCTURE ■ FUNCTION ■ BIOINFORMATICS

Characterization of a diagnostic Fab fragment binding trimeric Lewis X

Daniël C. de Geus,[1]* Anne-Marie M. van Roon,[1,2] Ellen A. J. Thomassen,[1] Cornelis H. Hokke,[2] André M. Deelder,[2] and Jan Pieter Abrahams[1]

[1] Biophysical Structural Chemistry, Leiden University, 2333 CC Leiden, The Netherlands
[2] Department of Parasitology, Leiden University Medical Centre, 2333 AZ Leiden, The Netherlands

ABSTRACT

Lewis X trisaccharides normally function as essential cell–cell interaction mediators. However, oligomers of Lewis X trisaccharides expressed by the parasite *Schistosoma mansoni* seem to be related to its evasion of the immune response of its human host. Here we show that monoclonal antibody 54-5C10-A, which is used to diagnose schistosomiasis in humans, interacts with oligomers of at least three Lewis X trisaccharides, but not with monomeric Lewis X. We describe the sequence and the 2.5 Å crystal structure of its Fab fragment and infer a possible mode of binding of the polymeric Lewis X from docking studies. Our studies indicate a radically different mode of binding compared to Fab 291-2G3-A, which is specific for monomeric Lewis X, thus providing a structural explanation of the diagnostic success of 54-5C10-A.

Proteins 2009; 76:439–447.

Key words: schistosomiasis; diagnosis; carbohydrate recognition; trimeric Lewis X; monoclonal antibody.

INTRODUCTION

Individuals suffering from schistosomiasis raise an immune response against a variety of schistosomal carbohydrate elements including Galbeta1-4(Fucalpha1-3)GlcNAcbeta (Lewis X, LeX), a trisaccharide that is expressed both in monomeric and polymeric form in different life stages of the schistosomes.[1] Schistosomiasis (originally named bilharzia) is the main human parasitic disease after malaria in tropical and subtropical areas. Infection occurs when cercariae, free-swimming larval forms of schistosomes or blood flukes, enter the human host through the skin during contact with infected surface water. After penetrating the body, the cercariae lose their typical forked tail and transform into schistosomula. This altered form of the parasite migrates via dermal veins to its final destination within the host's blood circulation, where it develops into male and female adult worms. Schistosomes have an average life span of 3–5 years (and may survive up to 30 years) in the hostile environment of their definitive host. Thus, this parasite must have developed remarkable mechanisms to escape the immune response of its host. It is thought that the glycoconjugates, which are abundantly expressed throughout all life stages of the parasite, play an important role in many of these escape mechanisms. Parasite glycans were found to induce immunomodulatory effects, for instance by downregulating the host-protective TH-1 type immune response or the induction of antiinflammatory responses.[2] Lewis X both in monomeric and oligomeric form is one of the glycoconjugates, which is abundantly expressed throughout the different life stages of the parasite.[3] Individuals with a schistosomal infection mount an immune response against the different oligomeric forms of Lewis X.[4–8] One of the antigens regularly released from the gut of adult worms, the circulating cathodic antigen (CCA), contains different oligomeric presentations of the carbohydrate Lewis X. Most of these presentations contain trimeric Lewis X (see Fig. 1) as part of a longer carbohydrate chain. CCA is excreted in such high amounts that sensitive assays to diagnose schistosomiasis are based on its detection in an ELISA using anti-Lewis X monoclonal antibodies. Recently, a reagent strip assay was developed containing anti-CCA Mab 54-5C10-A in its capture matrix, providing a simple and rapid alternative to the ELISA that can be used in endemic areas. The activity and intensity of a schistosomal infection can easily be measured by using this reagent strip based on the detection of CCA in the urine of patients.[9]

Abbreviations: CCA, circulating cathodic antigen; C_H1, constant heavy; C_L, constant light; FITC, fluorescein isothiocyanate; HSA, human serum albumin; IFA, immunofluorescence assay; SPR, surface plasmon resonance; TLS, translation, libration, and screw; V_L, variable light; V_H, variable heavy.

Anne-Marie M. van Roon's current address is Structural Studies Division, MRC Laboratory of Molecular Biology, Hills Road, Cambridge CB2 2QH, United Kingdom.
*Correspondence to: Daniël C. de Geus, Biophysical Structural Chemistry, Leiden University, Einsteinweg 55, 2333 CC Leiden, The Netherlands. E-mail: d.de.geus@chem.leidenuniv.nl
Received 6 May 2008; Revised 7 November 2008; Accepted 8 December 2008
Published online 23 December 2008 in Wiley InterScience (www.interscience.wiley.com). DOI: 10.1002/prot.22356

International efforts to generate antischistosome vaccines are part of schistosomiasis control programs.[10] Despite one potential candidate antigen (Sh28 GST) proceeding as far as Phase I and II clinical trials currently, no effective vaccine against the disease exists.[11] Although (medical) treatment with praziquantel cures up to 96% of the patients, reinfection easily takes place in most of the endemic areas.[11–14] A simple and rapid specific assay is therefore required, both for initial diagnosis and for the follow-up of chemotherapy.

In this article, as a contribution toward the immunology of schistosomiasis, we report an analysis of the characteristics of the diagnostically important antibody fragment 54-5C10-A. We show that it exclusively binds oligomeric Lewis X and not monomeric Lewis X. The crystal structure to 2.5 Å demonstrates a binding groove which is able to accomodate a trimeric Lewis X molecule. The structure of this trimeric LeX binding Fab is compared to the monomeric Lewis X binding Fab 291-2G3-A.[15]

METHODS

Purification of Fab 54-5C10-A

The murine Fab 54-5C10-A (IgG3κ isotype) was obtained from hybridoma cell culture supernatant using standard biochemical methods as described earlier.[16] During the purification, isoelectric focusing gel electrophoresis showed different isoforms of Fab 54-5C10-A with p*I* values of 9.3, 7.7, and 7. This mixture was dialyzed against 20 m*M* Tris-HCl pH 8 containing 0.02% (w/v) NaN_3 and loaded on an anion exchange column (UNO Q-1, Biorad). After elution with a 0-1*M* NaCl gradient the flowthrough containing the two isoforms with the highest p*I* values was dialyzed against 20 m*M* glycine buffer pH 9. However, these isoforms could not be separated by ion exchange chromatography, so the sample was concentrated to 15 mg mL^{-1} using an Ultrafree Centrifugal Filter Unit (Millipore) and used for crystallization.

Immunofluorescence assay

The immunofluorescence assay (IFA) was carried out on 6-μm thick sections of *S. mansoni* adult worms in frozen infected hamster liver tissue. Slides were incubated with Mab 54-5C10-A (25 μg/mL) in phosphate-buffered saline (PBS; 0.035*M* phosphate, 0.15*M* NaCl, pH 7.8), washed, and incubated with fluorescein isothiocyanate (FITC) labeled goat anti-mouse immunoglobulin according to manufacturer's instructions (Nordic, Tilburg, The Netherlands). Images were recorded using a Leica HC microscope equipped with a Leica DRC 350FX camera, using the appropriate filter combination for FITC fluorescence.

Surface plasmon resonance analysis of 54-5C10-A binding Lewis X-type neoglycoconjugates

Human serum albumin (HSA) neoglycoconjugates containing LNFPIII, di- or trimeric LeX were purchased from Isosep AB (Tullinge, Sweden) and contained on average 22 mol sugar per mol HSA. LNFPIII or lacto-*N*-fucopentaose III (Galβ1-4(Fucα1-3)GlcNAcβ1-3Galβ1-4Glcβ) is a pentasaccharide containing Lewis X at its nonreducing end. The BIAcore 3000 instrument, CM5 sensor chips, and an amino coupling kit were purchased from BIAcore AB (Uppsala, Sweden). The Lewis X neoglycoconjugates were immobilized on a CM5 sensor chip to a level of 7500 RU using the procedures described earlier.[15] Unmodified HSA was coupled on one flow channel of each sensor chip as a control. Five microliters of purified 54-5C10-A (1 mg mL^{-1} in 0.035*M* PBS) was injected. All analyses were performed, corrected, and evaluated as previously.[15]

Sequencing of the variable domains

Standard molecular biology protocols were used to synthesize and amplify cDNA of the IgG variable regions from total hybridoma mRNA.[15] The resulting DNA fragments were cloned in the pSTBlue-1 cloning vector according to the protocol of the Perfectly Blunt Cloning Kit (Novagen) and transformed into NovaBlue Singles Competent cells. Transformants were selected for the kanamycin resistance marker of the cloning vector and for the vector carrying an insert with X-Gal (5-bromo-4-chloro-3-indolyl-β-galactopyranoside). Sequences were obtained commercially (Base Clear, Leiden, The Netherlands) by automated dideoxy chain-termination technology using the T7 and SP6 promoter primers.

Crystallization and data collection

Prior to crystallization, the protein sample was filtered through a low-binding protein 0.22-μm filter (Millipore) to remove dust particles and protein precipitate. Crystallization trials were performed using the sitting drop vapor-diffusion technique at 295 K using equal volumes of protein and reservoir solution.

Data collection at cryogenic temperatures utilized crystals soaked in a solution containing 0.1*M* sodium citrate pH 4, 11% polyethylene glycol 3350 and 22.5% glycerol, flash-frozen in a stream of nitrogen gas at 100 K using an Oxford Cryosystems Cryostream device. Data were collected by the rotation method for 180 frames with 1.0° rotation and 25 s exposure time per frame, using a MAR Research 165 mm CCD detector on beamline BM14 at the European Synchrotron Radiation Facility (ESRF), Grenoble, France. The intensities were indexed using MOSFLM[17] and scaled using SCALA.[18]

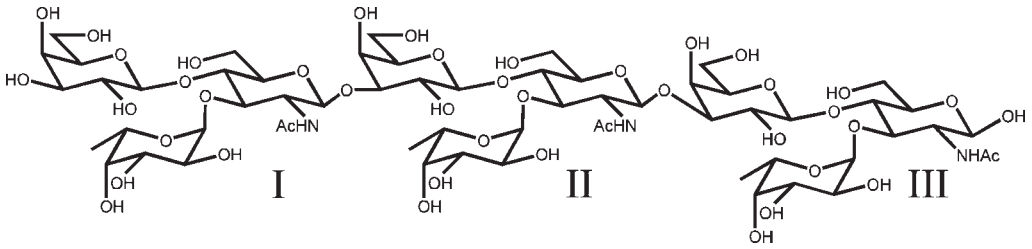

Figure 1

The antigen recognized by Fab 54-5C10-A is trimeric Lewis X. The repeating Lewis X units of the trimeric entity are labeled with Roman numerals.

Structure determination

The structure of Fab 54-5C10-A was solved by molecular replacement with MOLREP[19] from the CCP4 program suite[20] using the (uncomplexed) structure of the anti-monomeric Lewis X Fab fragment (PDB code 1UZ6) as a search model. The molecular-replacement solution was improved by rigid-body refinement and restrained refinement with REFMAC5.[21] Rebuilding was done with ARP/wARP[22] and Coot[23] and the refinement continued using TLS (translation, libration. and screw) parameters.[24] The quality of the final model with R_f = 0.20 and R_{free} = 0.26, was checked using PROCHECK[25] and WHATIF.[26] Illustrations were prepared using Pymol (Figs. 4 and 5; http://pymol.sourceforge.net/) and Accelrys DS Visualizer (Fig. 7; http://www.accelrys.com/).

Docking trimeric Lewis X into the binding groove

Currently no crystal structure is available for the trimeric Lewis X antigen (see Fig. 1); hence, a 3D model for this saccharide was generated using the program Sweet2.[27] The potential binding sites on the solvent accessible surface of one Fab 54 molcule (chain A and B) were determined with the grid-based cavity prediction implemented in the Molegro Virtual Docker (MVD) software (Molegro ApS, Aarhus, Denmark). The cavity corresponding to the antigen binding site was selected as the search space origin employing a 25 Å radius. Subsequently, the flexible ligand docking protocol of the MVD software was used and the resulting poses were imported back to MVD for visual inspection. The best pose, having the lowest scoring energy (the sum of the ligand–protein interaction energy and the internal ligand energy), was further analyzed.

RESULTS AND DISCUSSION

Screening antibodies for their meric Lewis X specificity

Previously, a large set of anti-schistosome monoclonal antibodies has been produced[28] and screened by SPR for their interaction with HSA Lewis X neoglycoconjugates.[29] Depending on their interaction behaviour Mabs were split up in three groups. Group I binds mono-, di- and trimeric Lewis X oligomers, group II interacts with both di- and trimeric Lewis X and group III has specific affinity for trimeric Lewis X. The sensorgrams of Mab 291-2G3-A (representing group I) and Mab 54-5C10-A (group III) shown in Figure 2 indicate that mono-, di- and trimeric Lewis X are immunologically discernible entities.

The natural epitope of Mab 54-5C10-A on adult worms *S. mansoni* worms is shown by immunofluorescence (see Fig. 3). Sections of schistosomes incubated with Mab 54-5C10-A and subsequently with FITC-labeled secondary antibody showed distinct fluorescent patterns in the gut of the worm.

Crystals and structure of the Fab fragment

Rectangular plate-shaped crystals of maximum dimensions 1.3 × 0.1 × 0.1 mm^3 were grown from 0.1*M* sodium citrate pH 4, 11% polyethylene glycol 3350. A single crystal was used for the data collection with data-processing statistics as shown in Table I. Analysis of the X-ray diffraction pattern indicated that along the k axis reflections were only present if $k = 2n$, identifying the space group as $P2_1$.

The Fab 54-5C10-A structure (later referred to as Fab 54) was determined to 2.5 Å resolution. The statistics of the final model (see Fig. 4) are shown in Table II. The framework region of the Fab 54 shows the usual immunoglobulin fold with elbow angles between the VL:VH and CL:CH1 pseudo-twofold axes of 134.6° (chain A,B) and 133.1° (chain E,F). Small elbow angles like these are the most preferred among κ chain type Fabs.[32]

Model quality of the native Fab 54 crystal structure

In the final model of Fab 54 with R_f = 0.20 and R_{free} = 0.26 the amino acid residues 126–132 of the heavy chain F (and 127–131 of heavy chain B) are missing. This region is located in a flexible loop with higher than

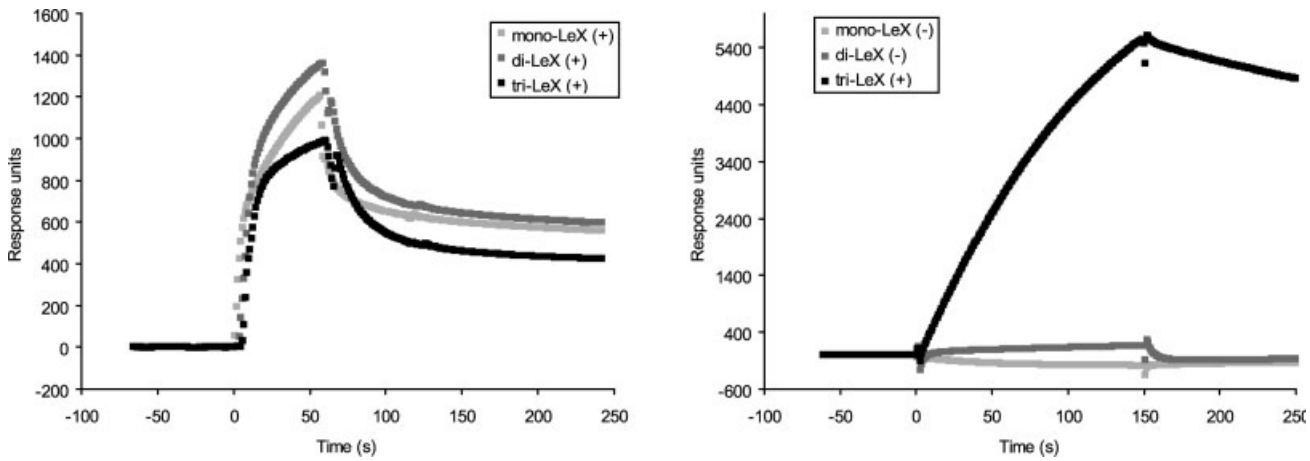

Figure 2

SPR sensorgrams of Mab 291-2G3-A (left) and Mab 54-5C10-A (right) with mono-, di- and trimeric Lewis X HSA-glycoconjugates. The interaction of the antibody was interpreted as binding (+) or non-binding (−).

average sequence variability according to the variability index for constant domain sequences and is often disordered in Fab crystal structures.[33] Extra density in the vicinity of the protein chain in the model was interpreted as glycine, azide, and glycerol molecules (used in the crystallization and cryoprotection). The structure of Fab 54 has 89% of all residues in the most favoured region, having less than 1% in the disallowed area of the Ramachandran plot. In both light chains, the residue Val L51 (Kabat numbering), which lies in a turn located between two β-strands at the beginning of CDR-L2, is a Ramachandran outlier. This is commonly observed in other Fabs.[34]

Analysis of the Fab 54 hypervariable loops: Sequence and structure

The Fab 54 structure showed a rather long and narrow cleft separating the hypervariable parts of the heavy and light chain [Fig. 5(a,b)]. The dimensions of this binding channel are ∼11 Å wide, 7 Å deep and 24 Å long (measured in Coot[35]) contrasting with the relatively small binding pocket of Fab 291 [Fig. 5(c)]. The latter accommodates the Lewis X trisaccharide in a pocket 13 Å wide, 10 Å deep, and 15 Å long.[15]

It is known that hydrogen bonds and van der Waals contacts are the most important factors in stabilizing protein–carbohydrate complexes[36] and sugar binding

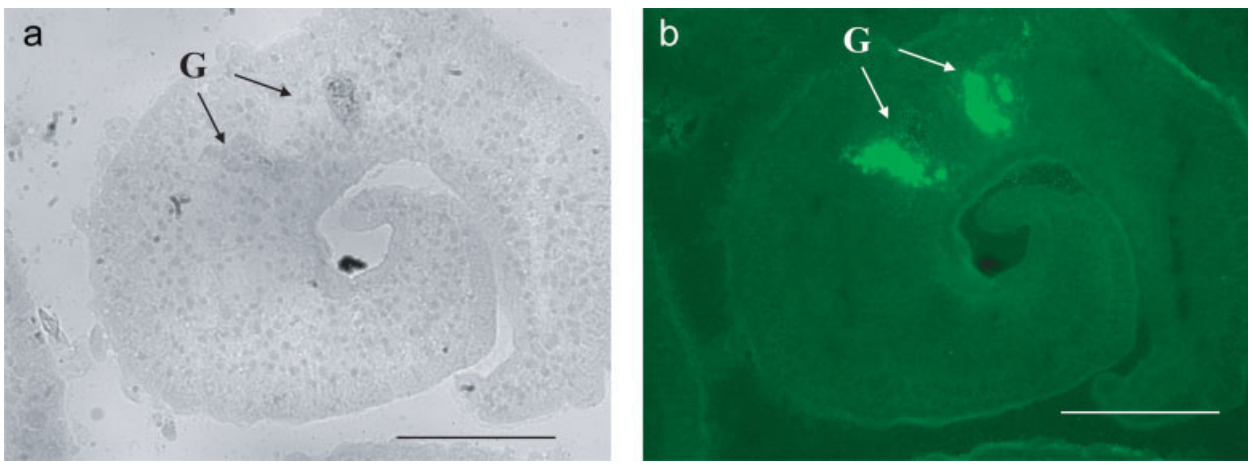

Figure 3

IFA: normal light (**a**) and immunofluorescence (**b**) microscopy image of a section of an adult S. mansoni worm incubated with Mab 54-5C10-A specific for the circulating cathodic antigen (CCA). Fluorescence is specifically observed in the gut (G) of the worm. Bar = ∼100 μm.

Table I
Data-Processing Statistics for the Fab 54-5C10-A Crystal

X-ray source	ESRF BM 14
Wavelength (Å)	0.95372
Resolution range (Å)	28.7–2.5 (2.64–2.5)[a]
Crystal system	Monoclinic
Space group	$P2_1$
Unit cell parameters (Å, °)	$a = 51.4$, $b = 161.0$, $c = 53.5$ $\beta = 103.1$
Observed reflections	109,380 (15,957)
Unique reflections	29,262 (4281)
Redundancy	3.7 (3.7)
Completeness (%)	99.9 (100.0)
Average $I/\sigma(I)$	10.6 (3.2)
R_{merge}[b] (%)	5.5 (23.5)
Solvent content (%)	42.7
V_M (Å^3/Da)[c]	2.2

[a]Data of the outer resolution shell are given in parentheses.
[b]$R_{merge} = \Sigma|I - \langle I\rangle|/\Sigma I$, where I is the integrated intensity of an observed reflection and $\langle I\rangle$ is the average intensity over symmetry-equivalent measurements.
[c]Matthews coefficient.[30]

Table II
Refinement Statistics for the Fab 54-5C10-A Crystal

Refinement	Fab 54-5C10-A
Resolution range (Å)	25.0–2.5
R-factor	0.203 (0.260)[a]
Number of Fab molecules in the AU	2
Number of TLS groups	28
Protein residues	848
Water molecules	214
Ligands	8 glycines/3 glycerols/1 azide
RMS deviations bonds (Å)	0.020
RMS deviations angles (°)	1.668
Average *B* value (Å^2)	
Protein/solvent	43.0/38.9
Glycerol/glycine/azide	51.6/47.0/46.1
Ramachandran statistics overall (%)	88.8/8.3/2.0/0.8[b]
A, B chain	89.6/8.7/1.1/0.5
E, F chain	88.0/8.2/2.7/1.1

[a]Data statistics of R_{free} are given in parentheses.
[b]Order: most favoured, additionally allowed, generously allowed and disallowed regions. The Ramachandran plot was generated with PROCHECK.[31]

sites are therefore usually populated by planar polar side chains partaking in hydrogen bond networks. Aromatic side chains can form additional hydrogen bonds with sugar residues [see Tyr B57 in Fig. 5(d)] and are able to stack with the hydrophobic face of the sugar ring.

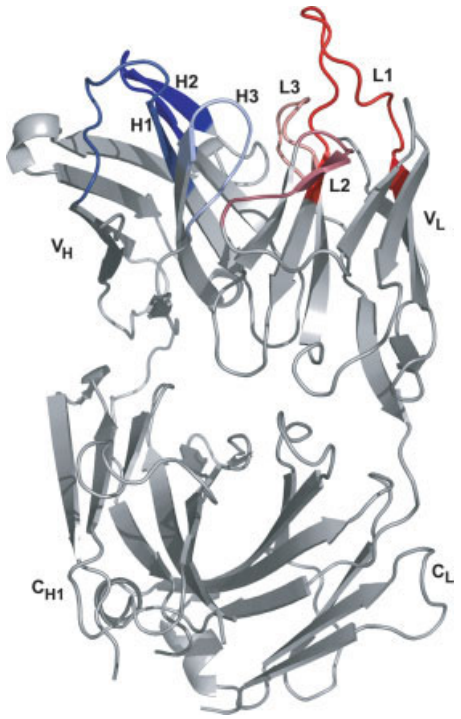

Figure 4
Ribbon representation of the Fab fragment 54-5C10-A. Complementarity determining regions of the light and heavy chain are depicted as CDR-L1 (red), L2 (raspberry), L3 (salmon) CDR-H1 (darkblue), H2 (blue) and H3 (lightblue).

Indeed, almost half of the binding site residues in Fab 54 have polar or aromatic side chains, but this fraction is identical in the case of Fab 291 (see Fig. 6), which binds a monomer of Lewis X only.

Analysis of the six CDRs in the Fab 54 sequence classified CDR-L1, L2 and L3 to the same structural clusters as the corresponding regions in Fab 291 (4/16A, 1/7A, and 1/9A, respectively), but the heavy chain CDRs belong to different classes for the two Fabs. CDR-H1 of Fab 54 is a class 3/12A and CDR-H2 a 1/9A loop (1/10A and 3/10B in Fab 291, respectively). Among the six CDRs, the H3 segment has a distinctive role in antigen recognition and the largest diversity in length, sequence and structure.[38–40] Based on the "H3-rules" describing the relationship between the sequence and the CDR-H3 conformation derived from crystal structures, the H3 loop of Fab 54 is predicted to be a kinked base.[40] Indeed the side chain of Asp H101 forms a salt bridge with Arg H94 at the start of CDR-H3. Fab 291 should also form the kinked base according to the H3-rules, but the protein model shows an extended structure, probably caused by the presence of the charge and size of Arg H99 and Phe H100.

Modeling trimeric Lewis X into the binding groove

We were not able to grow crystals containing the trimeric Lewis X antigen, neither using co-crystallization nor soaking. We decided to use docking as an alternative way to study and predict the Fab 54 interaction with trimeric Lewis X. The molecule in the asymmetric unit showing the best Ramachandran statistics (chains A and B) was selected and the flexible ligand docking protocol of MVD resulted in the optimal fit of the carbohydrate into the antigen binding site as shown in Figure 5(a,b,d). All three Lewis X moieties are in contact with the

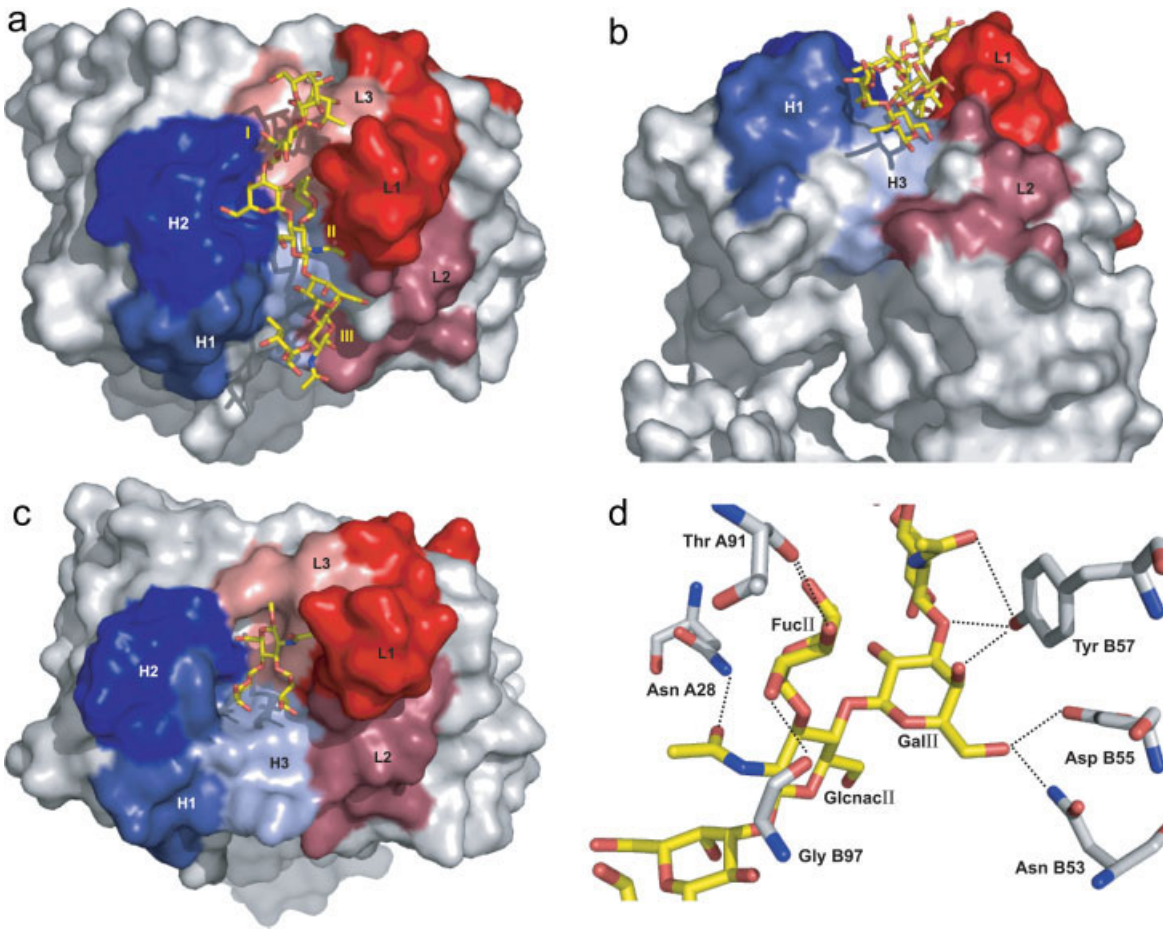

Figure 5

Comparison of two Lewis X binding sites. The complementarity determining regions of the light and heavy chain are depicted as in Figure 4. (**a,b**) Crystal structure of the light and heavy chain from Fab 54-5C10-A with trimeric Lewis X (yellow) docked into the antigen binding site. The repeating Lewis X units of the trimeric entity are labeled with Roman numerals as in Figure 1 and Table III (**c**) Crystal structure of the light and heavy chain from Fab 291-2G3-A in complex with monomeric Lewis X. (**d**) Close view of the docked trimeric Lewis X showing the intermolecular hydrogen bonding interactions. For reasons of clarity, only the central part of the carbohydrate chain is depicted.

antibody paratope, while the middle one seems to anchor with the most and tightest hydrogen bonds [Table III and Fig. 5(d)]. Binding of the trimeric Lewis X buries 822 Å^2 of the 19,170 Å^2 solvent accessible surface of one Fab molecule, whereas the monomeric Lewis X in the crystal structure of 291-2G3-A buries 302 Å^2 upon binding. In both cases, residues of all CDRs are involved in hydrogen bonds bridging the antigen. One striking feature of the Fab 54 binding groove is that it is dominated by aromatic residues like the binding pocket in Fab 291, but more extended over the entire binding surface. Aromatic stacking is observed for the Fab 54 amino acids residues Phe A32, which interacts with FucII, and Trp B52 with GalII.

Burial of nonpolar groups at the interface also contributes to the trimeric Lewis X binding affinity. The methyl group of the GlcNAcI acetyl function is stabilized by the side chains of Val A94 and Tyr B57, while the FucI methyl makes a van der Waals interaction with the Ser A27E OG atom. The Fab 291 light chain residue Tyr 27d, forming several hydrogen bonds and a van der Waals interaction with its monomeric antigen, has been replaced by His A27d in Fab 54 to make several van der Waals interactions with the FucII methyl group. Furthermore, Ser B32 and Gly B33 in Fab 54 are substitutes for the bulkier heavy chain residues Tyr 32 and Trp 33 of Fab 291. The Ser and Gly side chains create, in concert with Met B34, an intermediate hydrophobic surface stabilizing the methyl of FucIII. The overall hydrophobic character of the binding groove with a few flanking charges involved in hydrogen bonding, is shown in Figure 7.

The structure of the Lewis X trisaccharide is relatively rigid in solution, corresponding closely to the conformation

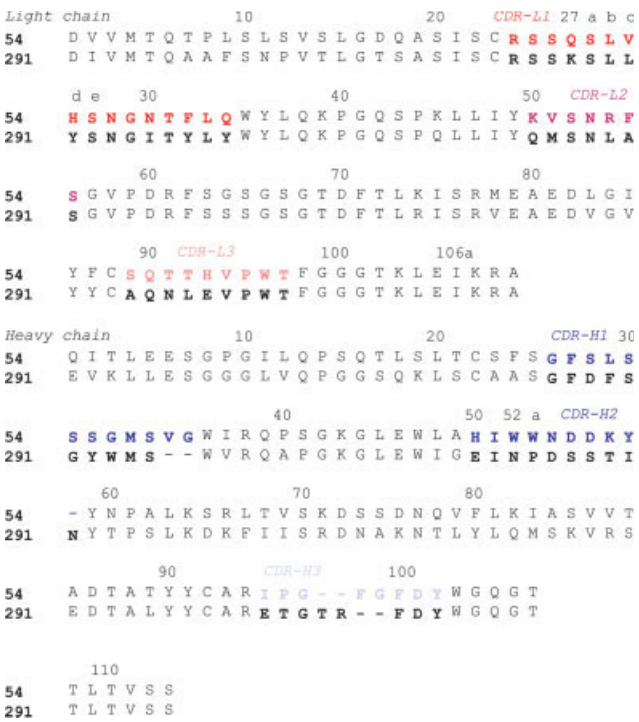

Figure 6

Sequence alignment of the variable part of the light and heavy chain of Fab 54 and Fab 291. CDRs (complementarity determining regions) are shown in bold and coloured as in Figures 4 and 5. Residue numbering is according to the Kabat numbering scheme and CDRs are defined following AbM definitions.[37]

found in the crystal structure. In general, the monomer is stabilized by stacking of the hydrophobic face of the fucose with the galactose ring. The structure of trimeric Lewis X is unknown, and therefore, the docked model has been analyzed by evaluating the torsion angles at the glycosidic linkages (see Table IV). The torsion angles were compared to those present in carbohydrate structures in the Protein Data Bank using GlyTorsion.[43] All torsion angles of the trimeric Lewis X model are in the range of most commonly observed angles for the Fucα(1-3)Glcnac linkage (of 214 torsions analysed), while the only outlier for the Galβ(1-4)Glcnac bond (of 120 torsions analysed) is Ψ1 of the third Lewis X unit. While the Lewis X units I and II resemble the monomeric Lewis X conformation in terms of torsion angles and hydrophobic stacking of the fucose with the galactose ring, the third Lewis X differs the most. Possibly the absence of hydrophobic stacking in this third unit is compensated by hydrogen bonds between GalIII and Lys A50 from the CDR-L2 and between FucIII and Ser B32 from CDR-H1.

The recognition site for the second Lewis X unit [Fig. 5(a)] is comparable in appearance to the monomeric binding pocket [Fig. 5(c)]. Despite this similarity, the mode of binding of the target is different. Lewis X unit II in Fab 54 is rotated ~180° in the binding groove compared to the monomeric Lewis X in Fab 291. The resulting orientation of Lewis X unit II is very similar to the binding mode of the Lewis X moiety in the crystal structure of the Fab BR96-nLewis Y complex. BR96 is a tumour selective antibody binding the nonoate methyl ester derivative of Lewis Y, a tetrasaccharide containing Lewis X.[44] The presence of at least three Lewis X units is essential for binding Fab 54 (see Fig. 2). The absence of one or two Lewis X units would leave a considerable part of the binding pocket unoccupied. It has been demonstrated

Table III

Hydrogen Bonds Between Trimeric Lewis X and the CDRs of Fab 54 (Kabat Numbering)

CDR	Fab 54-5C10-A residue	Atom	Distance (Å)	Sugar residue[a]	Atom
L1	Asn A28	ND2	3.2	GlcnacII	O7
L2	Lys A50	NZ	3.2	GalIII	O6
L3	Thr A91	O	2.7	FucII	O3
L3	Thr A91	O	2.7	FucII	O4
L3	His A93	ND1	2.9	FucI	O4
H1	Ser B32	O	3.2	FucIII	O4
H2	Asn B53	ND2	3.2	GalII	O6
H2	Asp B55	OD2	3.1	GalII	O6
H2	Tyr B57	OH	3.2	GlcnacI	O1
H2	Tyr B57	OH	2.6	GalII	O4
H3	Gly B97	O	2.6	FucII	O2

[a]Numbering of the sugar residues is according to the Lewis X units [indicated with Roman numerals in Figs. 1 and 5(a)].

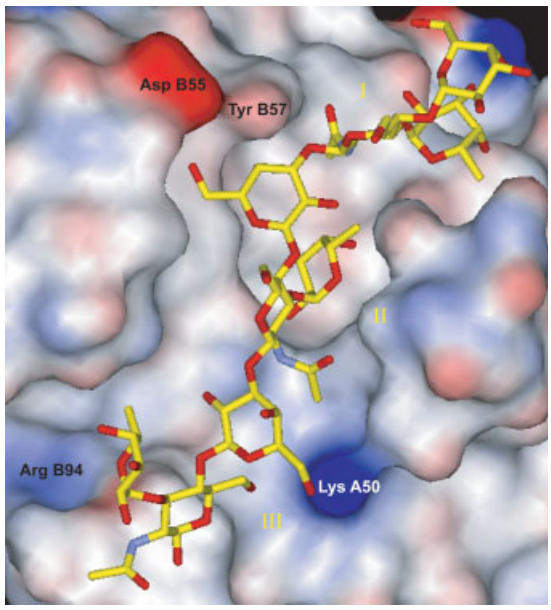

Figure 7

Molecular surface (colored according to electrostatic potential) for the Fab 54 binding site. Proximal residues with the largest charge are labeled.

Table IV
Comparison of the Torsion Angles[a] at the Glycosidic Linkages in Lewis X

	Torsion angle of trimeric Lewis X unit			Torsion angle of monomeric Lewis X in		
Linkage	I	II	III	Crystal[b]	Cocrystal[c]	Solution[d]
Galβ(1-4)Glcnac (Φ1/Ψ1)	−67.1/−118.4	−49.8/−72.8	−65.6/−58.8	−70.5/−107.7	−66.7/−114.4	−75/−104
Fucα(1-3)Glcnac (Φ2/Ψ2)	−59.1/155.2	−72.6/134.7	−58.6/149	−76.7/139	−82.7/136.7	−81/151

[a]Torsion angles are defined as Φ1 = O5gal-C1gal-O4glcnac-C4glcnac, Ψ1 = C1gal-O4glcnac-C4glcnac-C5glcnac, Φ2 = O5fuc-C1fuc-O3glcnac-C3glcnac and Ψ2 = C1fuc-O3glcnac-C3glcnac-C4glcnac.
[b]Values for one of the two molecules present in the asymmetric unit.[41]
[c]Lewis X conformation as observed in one of the two Fab291-Lewis X complexes present in the asymmetric unit.[15]
[d]Calculated lowest energy conformation.[42]

for the anti-tumor antibody BR96 that even the absence of one hexose unit of its tetrasaccharide antigen nLewis Y resulted in the disappearance of binding, while the one concerning hexose unit is interacting solely with one His residue in the BR96-nLewis Y complex.[45]

We anticipate that higher oligomeric forms than trimeric Lewis X might bind to Fab 54 as well. This requires a movement of CDR-H3 to convert the combining site from a 24 Å long channel into one sufficiently extended to accomodate additional Lewis X units. However, this is not unlikely to happen since structural changes of CDR-H3 side chains up to 15 Å movements are known.[46,47]

CONCLUSIONS

To better understand molecular recognition of trimeric Lewis X, we have determined the sequence and the structure of the anti-CCA Fab 54. The SPR results from this study clearly demonstrate that the described Fab 54 needs at least three repeating units of the Lewis X trisaccharide to bind CCA. We have docked this trimeric Lewis X ligand into the groove-type antigen binding site and conclude that all six CDRs contribute to binding. Together with the Fab 291-monomeric Lewis X structure, the current model provides a framework for understanding the specificity for the different Lewis X antigens involved in schistosomiasis. The crystal structures show a striking difference in the morphology of the antigen binding site: a long channel in Fab 54 in contrast to a rather shallow binding pocket in Fab 291. In addition, the crystal structure of this diagnostic Fab 54 fragment implies that a more extended, repeating epitope fits into its binding site. The current study has revealed the property of Fab 54 to recognize oligomers of at least three Lewis X units which enables the CCA detection from urine while excluding cross reactivity with shorter endogenous Lewis X fragments from the infected host.

Coordinates and sequences

Coordinates and structure factors have been deposited in the Protein Data Bank (accession code 2VQ1). The sequences of the variable domain of the heavy and light chain have been deposited in the EMBL/GenBank/DDBJ database (AM944590 and AM944591, respectively).

ACKNOWLEDGMENTS

We thank René van Zeyl for culturing hybridoma cells containing Mab 54-5C10-A and Hans de Vrind for his practical assistance with sequencing and purification. The European Synchrotron Radiation Facility (ESRF) staff at beamline BM14 is gratefully acknowledged for access to the synchrotron radiation source and assistance with station alignment.

REFERENCES

1. Hokke CH, Deelder AM, Hoffmann KF, Wuhrer M. Glycomics-driven discoveries in schistosome research. Exp Parasitol 2007;117:275–283.
2. Thomas PG, Harn DA, Jr. Immune biasing by helminth glycans. Cell Microbiol 2004;6:13–22.
3. Hokke CH, Deelder AM. Schistosome glycoconjugates in host-parasite interplay. Glycoconj J 2001;18:573–587.
4. Nyame AK, Pilcher JB, Tsang VC, Cummings RD. Schistosoma mansoni infection in humans and primates induces cytolytic antibodies to surface Le(x) determinants on myeloid cells. Exp Parasitol 1996;82:191–200.
5. Nyame AK, Pilcher JB, Tsang VC, Cummings RD. Rodents infected with *Schistosoma mansoni* produce cytolytic IgG and IgM antibodies to the Lewis x antigen. Glycobiology 1997;7:207–215.
6. Richter D, Incani RN, Harn DA. Lacto-*N*-fucopentaose III (Lewis x), a target of the antibody response in mice vaccinated with irradiated cercariae of *Schistosoma mansoni*. Infect Immun 1996;64:1826–1831.
7. van Remoortere A, van Dam GJ, Hokke CH, van den Eijnden DH, van Die I, Deelder AM. Profiles of immunoglobulin M (IgM) and IgG antibodies against defined carbohydrate epitopes in sera of *Schistosoma*-infected individuals determined by surface plasmon resonance. Infect Immun 2001;69:2396–2401.
8. van Remoortere A, Vermeer HJ, van Roon AM, Langermans JA, Thomas AW, Wilson RA, van Die I, van den Eijnden DH, Agoston K, Kerekgyarto J, Vliegenthart JF, Kamerling JP, van Dam GJ, Hokke CH, Deelder AM. Dominant antibody responses to Fucalpha1–3GalNAc and Fucalpha1–2Fucalpha1–3GlcNAc containing carbohydrate epitopes in Pan troglodytes vaccinated and infected with *Schistosoma mansoni*. Exp Parasitol 2003;105:219–225.
9. van Dam GJ, Wichers JH, Ferreira TM, Ghati D, van Amerongen A, Deelder AM. Diagnosis of schistosomiasis by reagent strip test for

detection of circulating cathodic antigen. J Clin Microbiol 2004; 42:5458–5461.
10. Hagan P, Doenhoff MJ, Wilson RA, Al Sherbiny M, Bergquist R. Schistosomiasis vaccines: a response to a devils' advocate's view. Parasitol Today 2000;16:322–323.
11. Lebens M, Sun JB, Czerkinsky C, Holmgren J. Current status and future prospects for a vaccine against schistosomiasis. Expert Rev Vaccines 2004;3:315–328.
12. Grover JK, Vats V, Uppal G, Yadav S. Anthelmintics: a review. Trop Gastroenterol 2001;22:180–189.
13. Ross AG, Bartley PB, Sleigh AC, Olds GR, Li Y, Williams GM, McManus DP. Schistosomiasis N Engl J Med 2002;346:1212–1220.
14. Wu GY, Halim MH. Schistosomiasis: progress and problems. World J Gastroenterol 2000;6:12–19.
15. van Roon AM, Pannu NS, de Vrind JP, van der Marel GA, van Boom JH, Hokke CH, Deelder AM, Abrahams JP. Structure of an anti-Lewis X Fab fragment in complex with its Lewis X antigen. Structure 2004;12:1227–1236.
16. van Roon AM, Pannu NS, Hokke CH, Deelder AM, Abrahams JP. Crystallization and preliminary X-ray analysis of an anti-LewisX Fab fragment with and without its LewisX antigen. Acta Crystallogr D Biol Crystallogr 2003;59(Pt 7):1306–1309.
17. Leslie AG. Integration of macromolecular diffraction data. Acta Crystallogr D Biol Crystallogr 1999;55:1696–1702.
18. Evans P. Scaling and assessment of data quality. Acta Crystallogr D Biol Crystallogr 2006;62(Pt 1):72–82.
19. Vagin AA, Teplyakov A. MOLREP: an automated program for molecular replacement. J Appl Crystallogr 1997;30:1022–1025.
20. Collaborative Computational Project Number 4. The CCP4 suite: programs for protein crystallography. Acta Crystallogr D Biol Crystallogr 1994;50:760–763.
21. Murshudov GN, Vagin AA, Dodson EJ. Refinement of macromolecular structures by the maximum-likelihood method. Acta Crystallogr D Biol Crystallogr 1997;53(Pt 3):240–255.
22. Perrakis A, Morris R, Lamzin VS. Automated protein model building combined with iterative structure refinement. Nat Struct Biol 1999;6:458–463.
23. Emsley P, Cowtan K. Coot: model-building tools for molecular graphics. Acta Crystallogr D Biol Crystallogr 2004;60(Pt 12 Pt 1): 2126–2132.
24. Winn MD, Isupov MN, Murshudov GN. Use of TLS parameters to model anisotropic displacements in macromolecular refinement. Acta Crystallogr D Biol Crystallogr 2001;57:122–133.
25. Laskowski RA, MacArthur MW, Moss DS, Thornton JM. PROCHECK: a program to check the stereochemical quality of protein structures. J Appl Crystallogr 1993;26:283–291.
26. Vriend G. WHAT IF: a molecular modeling and drug design program. J Mol Graph 1990;8:52–56.
27. Lutteke T, Bohne-Lang A, Loss A, Goetz T, Frank M, der Lieth CW. GLYCOSCIENCES.de: an Internet portal to support glycomics and glycobiology research. Glycobiology 2006;16:71R–81R.
28. Deelder AM, van Dam GJ, Kornelis D, Fillie YE, van Zeyl RJ. Schistosoma: analysis of monoclonal antibodies reactive with the circulating antigens CAA and CCA. Parasitology 1996;112:21–35.
29. van Roon AM. *Schistosoma mansoni*: Structural and Biophysical Aspects of Lewis X-Antibody Interactions, 2005 Thesis, Leiden University.
30. Stanfield RL, Zemla A, Wilson IA, Rupp B. Antibody elbow angles are influenced by their light chain class. J Mol Biol 2006;357:1566–1574.
31. Stanfield RL, Fieser TM, Lerner RA, Wilson IA. Crystal structures of an antibody to a peptide and its complex with peptide antigen at 2.8 Å. Science 1990;248:712–719.
32. Barbas CF, III, Heine A, Zhong G, Hoffmann T, Gramatikova S, Bjornestedt R, List B, Anderson J, Stura EA, Wilson IA, Lerner RA. Immune versus natural selection: antibody aldolases with enzymic rates but broader scope. Science 1997;278:2085–2092.
33. Emsley P, Cowtan K. Coot: model-building tools for molecular graphics. Acta Crystallogr D Biol Crystallogr 2004;60(Pt 12 Pt 1): 2126–2132.
34. Quiocho FA. Carbohydrate-binding proteins: tertiary structures and protein–sugar interactions. Annu Rev Biochem 1986;55:287–315.
35. Al Lazikani B, Lesk AM, Chothia C. Standard conformations for the canonical structures of immunoglobulins. J Mol Biol 1997;273: 927–948.
36. Chothia C, Lesk AM, Tramontano A, Levitt M, Smith-Gill SJ, Air G, Sheriff S, Padlan EA, Davies D, Tulip WR. Conformations of immunoglobulin hypervariable regions. Nature 1989;342:877–883.
37. Shirai H, Kidera A, Nakamura H. H3-rules: identification of CDR-H3 structures in antibodies. FEBS Lett 1999;455:188–197.
38. Lutteke T, Frank M, der Lieth CW. Carbohydrate Structure Suite (CSS): analysis of carbohydrate 3D structures derived from the PDB. Nucleic Acids Res 2005;33:D242–D246.
39. Jeffrey PD, Bajorath J, Chang CY, Yelton D, Hellstrom I, Hellstrom KE, Sheriff S. The X-ray structure of an anti-tumour antibody in complex with antigen. Nat Struct Biol 1995;2:466–471.
40. Hellstrom I, Garrigues HJ, Garrigues U, Hellstrom KE. Highly tumor-reactive, internalizing, mouse monoclonal antibodies to Le(y)-related cell surface antigens. Cancer Res 1990;50:2183–2190.
41. Schuermann JP, Henzl MT, Deutscher SL, Tanner JJ. Structure of an anti-DNA fab complexed with a non-DNA ligand provides insights into cross-reactivity and molecular mimicry. Proteins 2004;57:269–278.
42. Chi SW, Maeng CY, Kim SJ, Oh MS, Ryu CJ, Kim SJ, Han KH, Hong HJ, Ryu SE. Broadly neutralizing anti-hepatitis B virus antibody reveals a complementarity determining region H3 lid-opening mechanism. Proc Natl Acad Sci USA 2007;104:9230–9235.
43. Matthews BW. Solvent content of protein crystals. J Mol Biol 1968; 33:491–497.
44. Laskowski RA. PROCHECK; a program to check the stereochemical quality of protein structures. J Appl Crystallogr 1993;26:283–291.
45. Perez S, Mouhous-Riou N, Nifant'ev NE, Tsvetkov YE, Bachet B, Imberty A. Crystal and molecular structure of a histo-blood group antigen involved in cell adhesion: the Lewis x trisaccharide. Glycobiology 1996;6:537–542.
46. Imberty A, Mikros E, Koca J, Mollicone R, Oriol R, Perez S. Computer simulation of histo-blood group oligosaccharides: energy maps of all constituting disaccharides and potential energy surfaces of 14 ABH and Lewis carbohydrate antigens. Glycoconj J 1995;12: 331–349.
47. Martin AC. Accessing the Kabat antibody sequence database by computer. Proteins 1996;25:130–133.